Motor Imagery EEG Signals Marginal Time Coherence Analysis for Brain-Computer Interface

Md. Sujan Ali, Mst. Jannatul Ferdous
Department of Computer Science and Engineering,
Jatiya Kabi Kazi Nazrul Islam University, Trishal, Mymensingh-2224, Bangladesh

***Abstract*—The synchronization of neural activity in the human brain has great significance for coordinating its various cognitive functions. It changes throughout time and in response to frequency. The activity is measured in terms of brain signals, like an electroencephalogram (EEG). The time-frequency (TF) synchronization among several EEG channels is measured in this research using an efficient approach. Most frequently, the windowed Fourier transforms-short-time Fourier transform (STFT), as well as wavelet transform (WT), and are used to measure the TF coherence. The information provided by these model-based methods in the TF domain is insufficient. The proposed synchro squeezing transform (SST)-based TF representation is a data-adaptive approach for resolving the problem of the traditional one. It enables more perfect estimation and better tracking of TF components. The SST generates a clearly defined TF depiction because of its data flexibility and frequency reassignment capabilities. Furthermore, a non-identical smoothing operator is used to smooth the TF coherence, which enhances the statistical consistency of neural synchronization. The experiment is run using both simulated and actual EEG data. The outcomes show that the suggested SST-dependent system performs significantly better than the previously mentioned traditional approaches. As a result, the coherences dependent on the suggested approach clearly distinguish between various forms of motor imagery movement. The TF coherence can be used to measure the interdependencies of neural activities.**

Keywords*—Brain-Computer Interface (BCI); Electroencephalogram (EEG); Short-time Fourier Transform (STFT); Synchrosqueezing Transform (SST); time-frequency coherence

I. Introduction

Brain signals (EEG) can be used to build the Brain Computer Interface (BCI), which is a more convenient and affordable method. EEG signals are captured by spatially scattered scalp sensors. The connections between the various areas of the brain, which is the primary organ of the nervous system, are becoming important in BCI research. The various sensors record the EEG signals, and coherence analysis is used to determine how coherent the signals are [1, 2, 3]. Coherence is typically estimated using spectral methods such as a Fourier or wavelet [4] transform. Coherence analysis is challenging to implement because cerebral activity signals are inherently non-stationary. Although the time-dependent Fourier transform (STFT) is one approach to solving the issue, it has not been completely effective for the aforementioned reasons: one cannot guarantee the stationarity of brain signals during each brief time interval and two the Heisenberg uncertainty principle limits the resolution of time-frequency representation. Despite being a data-adaptive signal analysis technique, the mother wavelet basis function is used in the wavelet transform to decompose signals. The approach also has difficulty with time-frequency resolution, where the resolution of the frequency is greater at low frequencies and less so at high frequencies. Also, this method is founded on choosing a mother wavelet. Because the mother wavelet was arbitrarily chosen without being matched to the analyzing signal, that led to an inaccurate and irreversible breakdown.

When combined with the continuous wavelet transform (CWT), the technique, known as synchrosqueezing transform (SST) [5], produced astoundingly precise time-frequency depictions of nonstationary as well as nonlinear data. This aspect of SST addresses the drawbacks of linear perception time-frequency techniques, such as windowed Fourier transforms (STFT) as well as continuous wavelet transforms. The synchrosqueezing transformation focuses the coefficient values around the frequency response graph of the tuned oscillations by dispersing the STFT and CWT strengths [6]. The frequency redistribution approach used in time-frequency representation [7] improves the proper location of instantaneous amplitude in the time and frequency domains.

Since neural synchronization is characterized by several frequency bands but is anticipated to change over time, TF coherence is typically employed for measuring it. Smoothing the cross as well as auto-spectra between the signals is essential since noise has a significant impact on coherence. One of the following techniques is used to execute the smoothing operation: periodogram smoothing can be accomplished in one of three ways: (i) Periodogram smoothing through ensemble averaging using the WOSA (Welch's overlapped segment averaging) technique; (ii) the temporal or frequency domains may be smoothed separately or together [8, 9]; and (iii) By averaging a collection of spectra generated using various orthogonal taper functions, cross and auto spectra are smoothed. The cross and auto spectra are typically smoothed with the same smoothing agents in all of the approaches mentioned above to estimate TF consistency. The employment of the same smoothing operator constrained the coherence to the range [0, 1] since the TF coherence satisfies the Cauchy-Schwarz inequality. Furthermore, the estimator using the same operation fails when the smoothing coefficient rises to one. Selected auto spectra smoothing can be used to get the improved temporal resolution. However, since the cross spectra are therefore not flattened when non-identical smoothing operators are used, the bias of the

estimator cannot reach one [8]. As a result, the estimator has better time resolution. In order to properly depict TF consistency and uncover weak correlations among signals, non-identical smoothing agents may be used. Bispectrum-based channel selection (BCS) was employed in this study [10] for MI-based BCIs. In this paper [11], the performance of the BCI model may be considerably impacted by using different time segments for training the data. They recommend against using any other temporal data as training data besides that utilized for motor imaging. For BCI Competition IV 2a and 2b, models using machine learning and deep learning suggested a potential improvement in visual display time, categorization efficiency. It was argued that models might be picking up more visual information. In fact, during the visual presentation, spatial topography revealed activation of the visual cortex. In the research [12], MI classification using EEG signals is accomplished using a supervised feature selection method. Another work [25] suggests a technique for producing a spatio spectral feature representation that can maintain the multivariate information of EEG data. In particular, subject-optimized and subject-independent spectrum filters were combined, and the filtered data were then stacked into tensors to create 3-D feature maps. In order to automatically choose the best frequency bands based on MIF [13], the MIFCSP method combines multivariate iterative filtering (MIF) and CSP. This method may then be used to extract discriminant features.

The SST approach is employed in the present study to calculate the TF coherence of brain signals, as well as the coherence is therefore subjected to a non-identical smoothing procedure. Moreover, the same analysis is carried out using the short-time Fourier transform rather than the SST. With synthetic and actual EEG signals, both findings are validated. The SST-dependent TF consistency outperforms the STFT-dependent technique, according to the observation in both synthetic and real data. The following is how the paper is set up: The time-frequency representation techniques, such as STFT and SST, are covered in Section II, along with the consistency in the TF domain in Section II, the synchronized transformation research findings in Section III, and discussion and some closing thoughts in Sections IV and V, respectively.

II. METHODS

The neuronal synchronization changes both over time and with frequency. Any signal's energy is described as a function of both times as well as frequency by the time-frequency representation (TFR). It converts a single-dimensional time-series signal through a double-dimensional function integrating frequency and period. The TFR space value gives a sense of which spectral components are present. Non-stationary or time-varying signals can be analyzed and created using the TFR.

A. Windowed Fourier Transform

An approach that works well for the TF characterization of non-stationary EEG signals is the short-time Fourier transform (STFT). A kind of trade-off between a signal's time and frequency is made by the STFT, which contains all the data on frequency variations with the period. A signal event's timing and frequency are also disclosed through this information. The signal is broken up into manageable chunks for the duration of the STFT, and it may be expected that each of these chunks will remain stationary. A window function (w) is selected in order to achieve this. This window must have the same width as the area of the signal when the normality of the data is guaranteed. The definition of the STFT for a non-stationary signal s(t) is

$$\Psi(t, f) = \int_{-\infty}^{\infty} [s(t).w^*(t-t')].e^{-2\pi f t} dt \quad (1)$$

where even the window function $w(t)$ and the complex conjugate * are both present. The signal's STFT is the signal's Fourier transform times a tapering function [27].

In the interests of demonstrating the time-frequency depiction, a noise-free artificial signal is created that is called δ(t) by chaining three sinusoids s1(t), s2(t), and s3(t) with frequencies of 10Hz, 5Hz, and 20Hz, respectively, with the formula as δ(t) = [s1(t) s2(t) s3(t)]. For sampling, 500 hertz (Hz) is employed. The STFT-based synthetic signal and TFR are shown in Fig. 1(a) and 1(b), respectively. A Hamming window with a 50% overlap and a length of 256 is employed in the STFT. Although with poor resolution, the STFT can distinguish between the three factors.

B. Synchronized Transformation

A useful method for the Continuous Wavelet Transform (CWT) is the Synchrosqueezing Transform (SST). This method is employed to concentrate the frequency elements of non-stationary signals in the TF space. The CWT successfully creates a high-resolution TF representation. In Fig.1, the SST-dependent TF visualization derived from the artificial signal *δ(t)* is displayed. The right CWT scales are used for discretization, and a bump mother wavelet is used to achieve SST. It has been highlighted that STFT-based TF space suffers from extremely poor frequency resolution and reduced temporal resolution owing to the employment of the window function. Using a set of wavelets, which are time-frequency filters, the CWT method detects oscillatory elements in a signal. The CWT is used to create wavelets from a successive time function. In the following form, a signal *s(t)* is convolved with a mother wavelet *Φ(t)*, which is a finite oscillatory consequence.

$$Z(p,q) = \frac{1}{|p|^{1/2}} \int_{-\infty}^{\infty} \Phi(\frac{t-q}{p}) s(t) dt \quad (2)$$

If each scale-time duet's (p,q) wavelet coefficients are represented by Z(p,q), then it is possible to determine the instantaneous frequency $\omega_s(p,q)$ by using the formula

$$\omega_s(p,q) = -iZ(p,q)^{-1} \frac{\partial Z(p,q)}{\partial q} \quad (3)$$

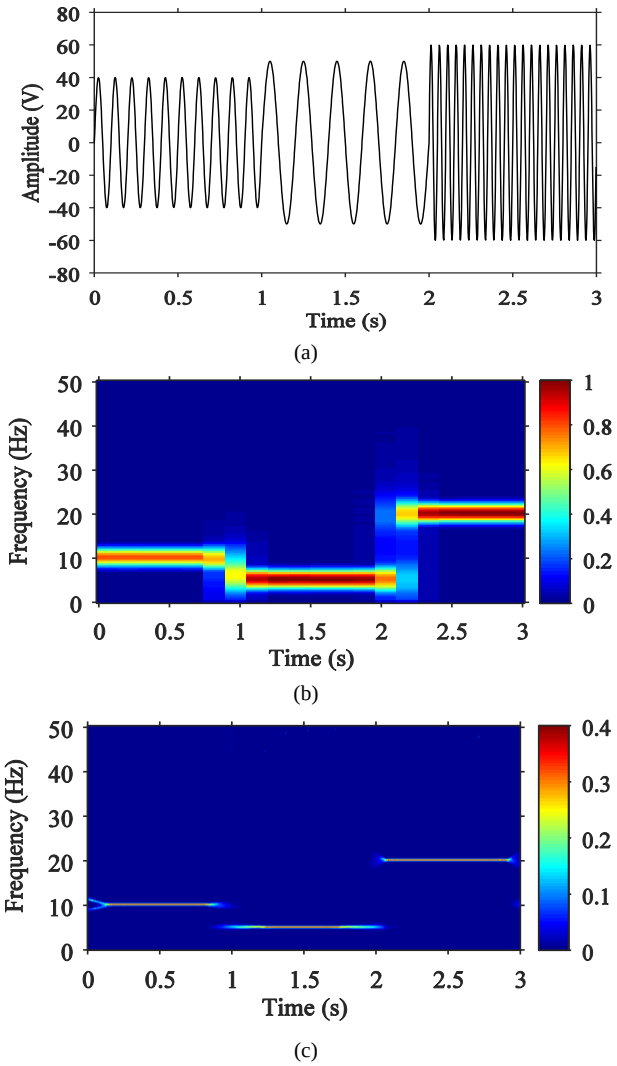

Fig. 1. A synthetic signal δ(t) with three sinusoids is represented by TF utilizing (a) the simulated signal δ(t) and (b) STFT as well as (c) SST.

With TF representation, the information from the time-scale frame is translated to the time-frequency frame. During the synchrosqueezing procedure, each value is changed to $(q,\omega_s(p,q))$ [5]. It is able to have a scaling step because p and q are distinct numbers; for each, p_k , where $\omega_s(p,q)$ is calculated. When projecting from the time-scale frame to the time-frequency frame $(q,p)\rightarrow(q,w_{inst}(p,q))$, the SST $\Gamma(\omega_l,q)$ is only calculated [11] in the centres ω_l located in the spectral region $[\omega_l-\Delta\omega/2,\omega_l+\Delta\omega/2]$ with $\Delta\omega=\omega_l-\omega_{l-1}$.

$$\Gamma(\omega_l,q)=\sum_{p_k:\left|\omega_s(p_k,q)-\omega_l\right|\le\Delta\omega/2} Z(p_k,q)p^{-3/2}\Delta p_k \tag{4}$$

Eq. (4) demonstrates that only the frequency (or scale) axis is synchrosqueezed in the TF representation of the signal [14, 28]. To obtain a focused image over the time-frequency plane for the SST, the CWT coefficients are reallocated [15]. The instantaneous frequencies are then taken from this image.

C. Coherence Evaluation

Effective communication between two parties can be achieved through coherence. Cohesiveness in neuroscience describes the systematic constancy among two neuronal cells. The establishment of more or less uniformity between oscillating modulations in different neurons' brain activity is known as neuronal coordination. Synchronization has a substantial impact on how the different neuronal regions synchronize their stimulatory behavior [16, 17, 18].

D. Frequency Coherence

A common technique for assessing consistency within brain waves is frequency consistency. Frequency coherence's major benefits include being highly implicit, hard, and noise-resistant while allowing for a quick overview of pertinent consistent frequencies in the sample [19]. The frequency coherence is a measure of how well multiple signals' cross-spectral levels hold up when normalized with respective auto-spectral levels. As functions of frequency, consider *x* and *y*, two stationary random processes. According to [26], the familiar consistency function of x, as well as y, is as follows:

$$\left|C_{x,y}(f)\right|=\frac{\left|J_{x,y}(f)\right|}{\sqrt{J_{x,x}(f)J_{y,y}(f)}} \tag{5}$$

wherever $J_{x,y}(f)$ is the cross-spectral density among the two processes. $J_{x,x}(f)$and $J_{y,y}(f)$ are the auto spectral density functions of *x* as well as *y*, respectively, at frequency, *f*. The EEG is a non-stationary signal; hence the conventional coherence function is insufficient.

E. Coherence of Time and Frequency

Typically, coherence analysis only works with stationary signals since it calculates the relationship between two signals throughout the frequency region. Consequently, much like with non-stationary signals, traditional coherence analysis is unable to reveal the temporal features of EEG [20]. The sequential relationship among both processes in the time-frequency dimension is measured using an advanced ruling technique. The TF consistency has been employed to gauge the synchronization of cortical activity in the brain-computer interaction motor imagery experiment. The coherence characteristic of the TF is described as

$$\left|C_{x,y}(t,f)\right|=\frac{\left|J_{x,y}(t,f)\right|}{\sqrt{J_{x,x}(t,f)J_{y,y}(t,f)}} \tag{6}$$

At this point, $t=1,2,\ldots,T$; $f=1,2,\ldots,$ is the distinct frequency and the signal is divided into *T* segments. The measurements of the sectional as well as auto-spectral concentrations are

$$J_{x,y}(t,f)=X(t,f).Y^{*}(t,f)$$
$$J_{x,x}(t,f)=\left|X^{2}(t,f)\right|,\qquad J_{y,y}(t,f)=\left|Y^{2}(t,f)\right| \tag{7}$$

where $X(t,f)$ and $Y(t,f)$ are the respective x also y of TF transforms coefficients, besides $Y^*(t,f)$ is the complex quantity of $Y(t,f)$.

The TF consistency definitions are simple and also use a method akin to the Fourier analysis. Based on the spectrogram approach, which involves averaging the signal segments to arrive at the estimates, the spectra and the frequency coherence in the Fourier analysis can be calculated. As both time and frequency have two dimensions, the time-frequency consistency encounters challenges throughout averaging. SST, which performs better than STFT, is used throughout this study to compute the TF translation parameters accompanied by TF consistency

F. Smoothing Impacts on TF Coherence

To get rid of noise, utilize the smoothing operator, and a convolution operator. The operators for smoothing cross- and auto-spectral densities can be the same or different. The employment of non-identical operators, as opposed to identical operators, produces time-frequency consistency that is unrestricted to [0, 1] and, as a result, improves temporal resolution [8]. Smoothing both time and frequency is necessary to increase the TF coherence's constancy. Averaging a number of orthogonal-based spectrum estimations, such as those obtained using multi-taper methods, can serve as the smoothing operator. They are typically employed for amplitude- and auto-spectral densities. The non-identical smoothing agents are two-dimensional in both time and frequency [21] or a single-dimensional function of time. Thus, the standard magnitude squared TF coherence is calculated as [8]

$$\left|C_{x,y}(t,f)\right|^2 = \frac{\left|J_{x,y}(t,f)\otimes w[\phi]\right|^2}{\left\{J_{x,x}(t,f)\otimes w[\varphi]\right\}\left\{J_{y,y}(t,f)\otimes w[\varphi]\right\}} \quad (8)$$

Here, $w[\phi]$ also $w[\varphi]$ remain two different ($w[\phi]\neq w[\varphi]$)) leveling windows of cross-spectral concentration and auto spectral concentration, accordingly, and $\otimes$ denote the convolution operator. The impacts of smoothing in TF consistency are demonstrated in Fig. 2, where two artificial signals x_1=[sin($2\pi f_1 t$) sin($2\pi f_2 t$)], x_2=[sin($2\pi f_1 t$) sin($2\pi f_2 t$)] with f_1=5Hz also f_2=10Hz and their TF consistency remain accessible. According to Fig. 2(a) and 2(d), respectively, the individual sinusoids that make up x_1 and x_2 have various temporal lengths.

As shown in Fig. 2(e), and 2(f), smoothing operations are shown to increase the TF coherence's representativeness and clarity for both STFT and SST-based methods. On the other hand, as seen in Fig. 2(b) and 2(c), when the smoothing procedure is not carried out, a significant amount of irrelevant coherence is introduced. Hence, the measurement of time-frequency coherence is enhanced by utilizing diverse smoothing agents. Several 2-D Gaussian smoothing windows with various lengths are employed in this research. The kernel's height in hertz and width in seconds are denoted by h and d, respectively, to reflect the window length $w=[h \quad d]$.

G. Proposed Algorithm for TF Coherence

The steps that make up the suggested technique for calculating the time-frequency coherence amongst two signals dependent on SST are as follows:

1) Choose two EEG channels or two brain signals at random.

2) The time-frequency coefficients can be obtained by applying the SST to each individual signal.

3) The cross and auto spectral distributions should be calculated using the SST coefficients.

4) Using two acceptable non-identical (various window lengths) smoothing processes, amplify the cross and auto spectral densities.

5) Lastly, use Eq. (8) to get the time-frequency coherence by using smoothed auto and cross-spectral densities.

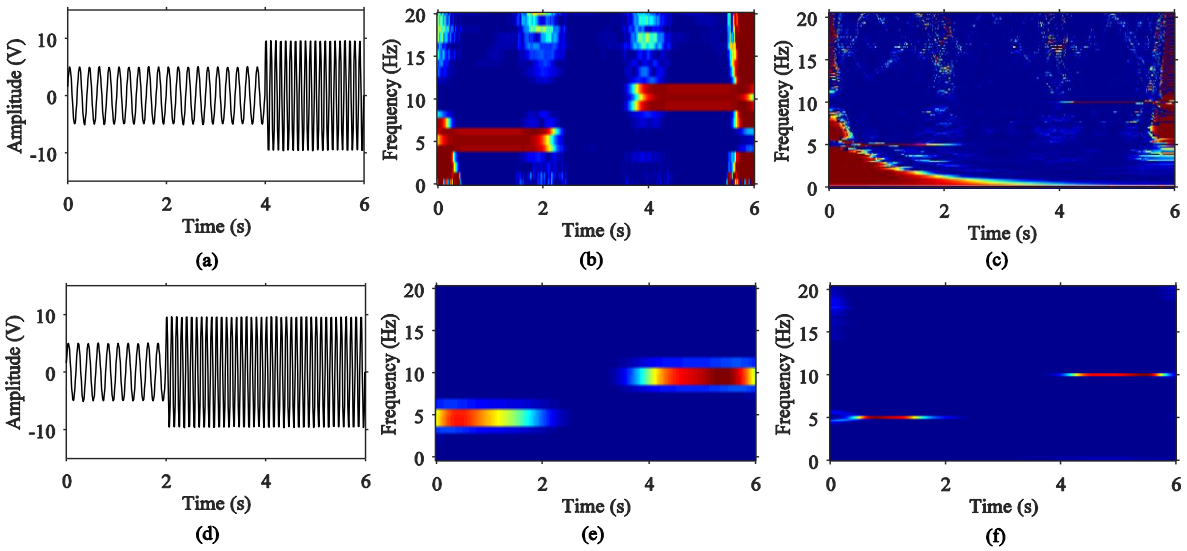

Fig. 2. The impact of smoothing operations on the TF consistency among the artificial signals x1 (a) as well as x2 (d). (b) STFT and (c) SST dependent TF lacking levelling, STFT and I STFT and (f) SST-dependent TF consistency through smoothing.

III. RESULTS

Both real EEG data and synthetic signals are utilized to evaluate the performance of the proposed SST-based time-frequency consistency. The outcomes are contrasted with time-frequency consistency dependent on STFT. With regard to STFT, a hamming window of length 100 is employed. Then, using non-identical smoothing windows, the spectral coefficients are smoothed for the calculation of TF coherence. The cross- and auto-spectral concentrations are levelled with Gaussian smoothing windows with lengths of w [2 1] and w [10 1], respectively. To execute the SST, a mother wavelet with bumps is utilized, and then the CWT scales' discretization is set at 32. The cross-spectral density is smoothed over in the SST because the Gaussian smoothing windows are w [3 1] and w [50 1] long. The Gaussian smoothing windows in the SST have lengths of w [3 1] and w [50 1], meaning that the cross and auto spectral densities are flattened across TF areas of 3 Hz and 1 s, respectively.

1) Synthetic data: Three sinusoids with frequencies of 5 Hz, 6 Hz, and 10 Hz are added together with a sampling frequency of 100 Hz to produce the trio of non- generated signals X, Y, and Z. As shown in Fig. 3, each of the simulated signals are made up of such three signals with various temporal alignments. The distinct synthetic waveforms X, Y, and Z are then each polluted with 5 dB, 0 dB, and -5 dB of Gaussian noise, accordingly. Fig. 4 and 5 show the time-frequency consistencies within each couple of artificial signals produced by STFT and SST, separately. The consistency among the signals Y and Z (5Hz and 6Hz frequency) is displayed in Fig. 4. while Fig. 5 shows the cohesiveness between the exact same pair of signals is separated in a more pronounced manner, they overlapped each other. Fig. 6, which shows the marginal frequency coherences of two approaches, exemplifies the phenomena clearly (STFT and SST). If f=1,2,...,F, the definition of the marginal frequency coherence is $\tilde{C}_{x,y}(f) = \sum_{t=1}^{T} \left| C_{x,y}(t,f) \right|^2$. In STFT, values for closer frequency coherence values overlap, whereas, with SST, the coherence of each individual frequency component is strongly represented. It is believed that the SST-based technique has better resolution than the STFT-based time-frequency coherence technique.

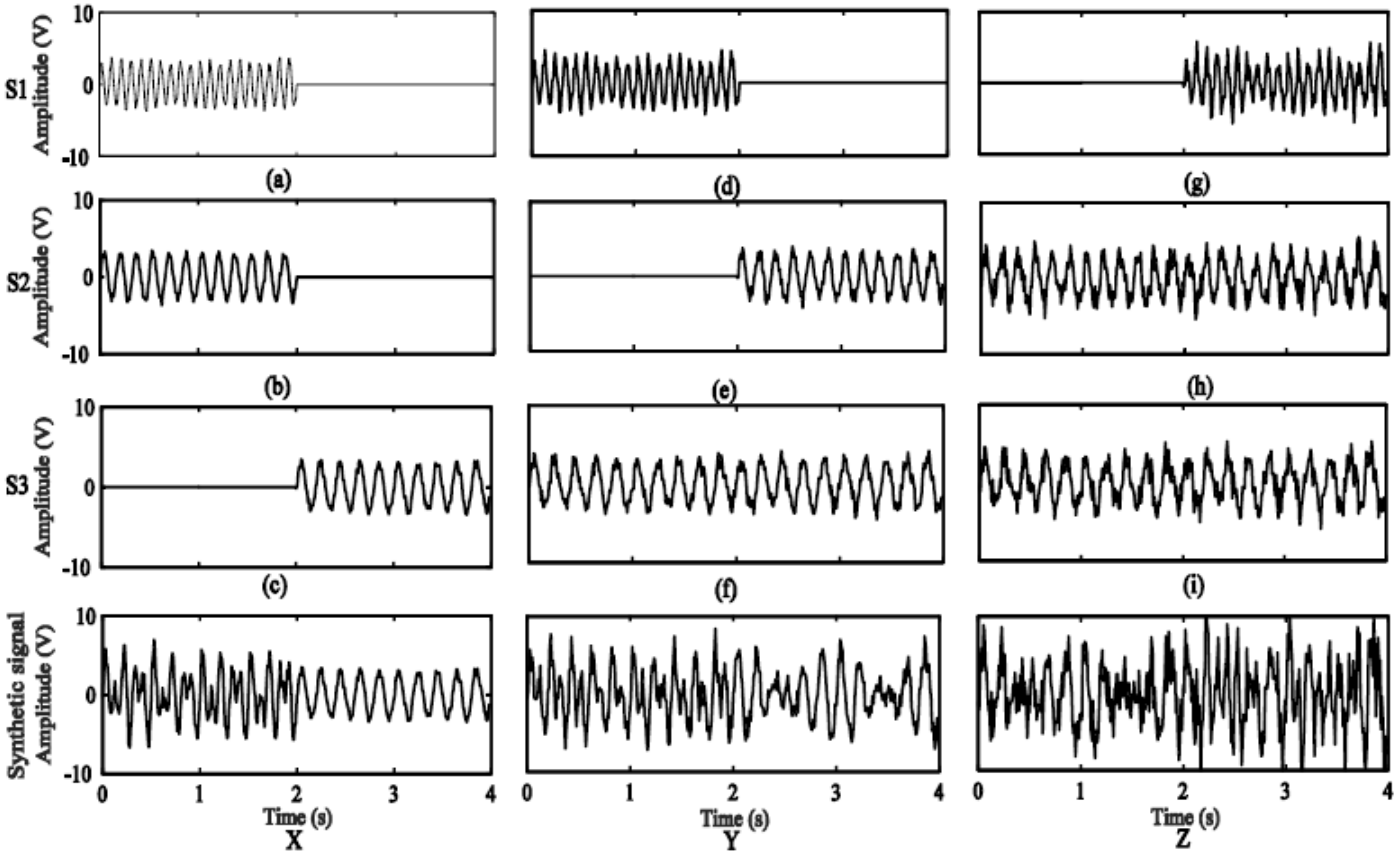

Fig. 3. Development of a multiple non-stationary [X, Y, Z] signal. Three separate frequencies sinusoids are present within the initial three rows (S1, S2, as well as S3). The three sinusoids in S1, S2, and S3 have, correspondingly, 10 Hz, 6 Hz, and 5 Hz frequency properties. To produce the artificial signals X, Y, and Z, alternative time alignments of the sinusoids are used. 5dB, 0dB and -5dB noises are inserted to sinusoids (a) to (c), (d) to (f) and (g) to (i) correspondingly. The synthesized signal in the fourth row is made up of the three sinusoids; X=(a)+(b)+(c), Y=(d)+I+(f) and Z=(g)+(h)+(i).

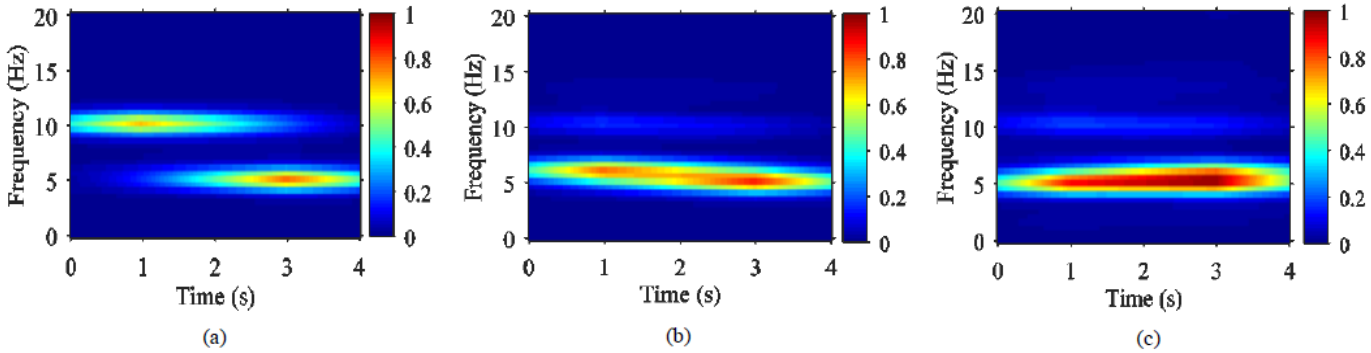

Fig. 4. Artificial signal STFT-depended TF consistency among (a) X and Y, (b) X and Z, and (c) Y and, Z.

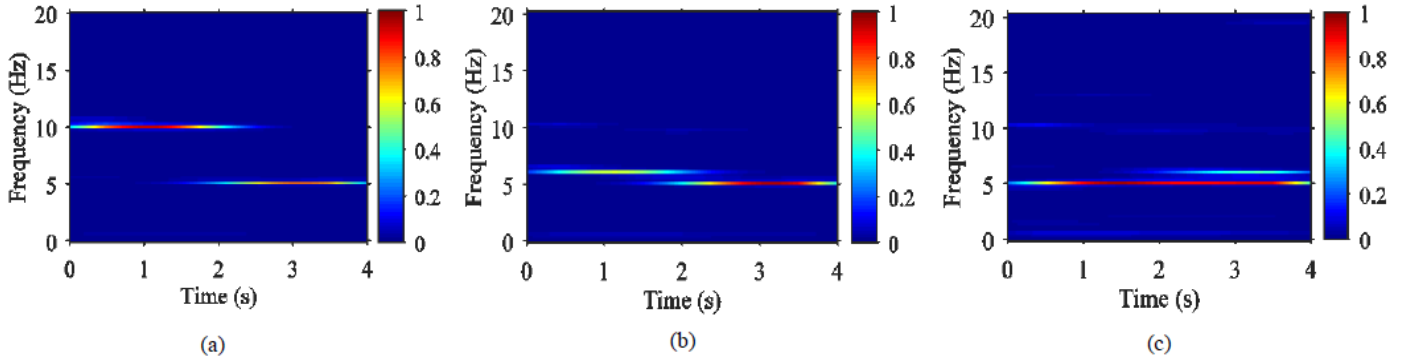

Fig. 5. Artificial signal coherence (a) between X as well as Y, (b) between X and Z, and (c) between Y and Z using SST-dependent TF.

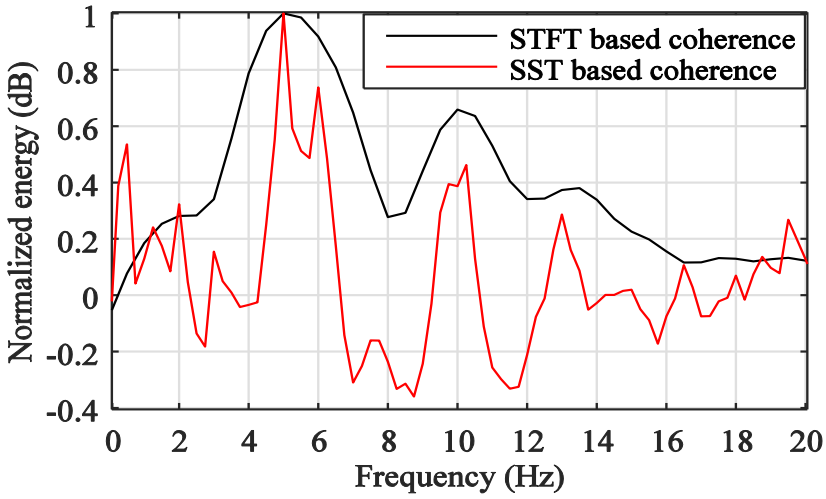

Fig. 6. Marginal frequency consistencies of STFT-depended coherence (black line) with SST-depended coherence (red line) between the artificial signals Y and Z.

2) Real data: The actual EEG data was gathered from the calib_ds1a. (IV dataset) generated from the 4th Brain-Computer Interface (BCI) Competition, which is openly accessible. The information is used to determine how well the suggested strategy performs. It is noted in subjects who are in good health. Motor imagery is accomplished during the entire session without any input. Two kinds of motor images are chosen from left hand, right hand, and foot movement for each subject. Movement signals of the left hand and foot are present continuously in the calibration dataset calib_ds1a. 59 EEG channels comprising 200 trials lasting four seconds each make up the data. The data are sampled at a rate of 100 Hz. The data offset from the EEG signals has been eliminated during pre-processing. In order to get the alpha frequency band, which has intricate patterns of intermittent synchronization, The brain wave then goes across a 4th-order

Butterworth band transfer filter with a frequency range of 8 Hz to 12 Hz. [8]. The inter-channel coherence is measured in this experiment using the two channels T7 and T8. Fig. 7 shows the unprocessed EEG signal, the purified alpha ingredient, as well as the spectrum of alpha for the left-hand movement channels T7 and T8. The foot movement data from channels T7 and T8 are similarly depicted in Fig. 8. The STFT-based time-frequency coherence for left hand and foot movement motor images are shown in Fig. 9(a) and 9(c) for channels T7 and T8. The time-frequency coherence between channels T7 and T8 of left hand and foot movement, based on SST, are shown in Fig. 9(b) as well as 9(d), correspondingly. Fig. 9 shows how SST-based TF coherence, in contrast to STFT, exhibits remarkable localization of extremely small band frequency components.

3) BCI interpretation: In this investigation, the time-frequency coherence across channels in the left and right hemispheres of the human brain, is investigated. Moreover, the distinction involving left hand and left foot action in motor imagery is seen. Sensorimotor rhythms can be managed with the help of motor imagery [22], and the patterns are more active in the central region of the brain [23]. The 59 EEG channels are therefore divided into three channels from each hemisphere (T7, FC5, and CP5) and three channels from each hemisphere (T8, FC6, and CP6) for coherence assessment. Fig. 11 depicts the spatial distribution of the scalp's channels in the 10/20 EEG system. To evaluate time-frequency coherences, there are eight-channel clusters used: FC5FC6, FC5T8, FC5CP6, T7FC6, T7T8, T7CP6, CP5FC6, CP5T8, as well as CP5CP6. On every one of the chosen channel pairings, time-frequency coherences based on STFT and SST are assessed. Eq. (9) determines how to weight the time-frequency coherences

$$\left|C_{x,y}(t,f)\right|^2_{weighted} = \left|C_{x,y}(t,f)\right|^2 \bullet \tilde{C}_{x,y}(f) \quad (9)$$

Here, the weight matrix is the marginal frequency coherence and the notation $\bullet$ is a binary singleton multiplication function. Using the weighted time-frequency coherence, the marginal time coherence is computed. It is said that minimal time coherence is

$$\tilde{C}_{x,y}(t) = \arg\max_f\left(\left|C_{x,y}(t,f)\right|^2_{weighted}\right); t = 1,2,3,\ldots,T \quad (10)$$

The minimal time consistency in this study is determined by averaging the marginal time coherence throughout 100 trials. The normalized readings during the time for several connection pairs of left-hand and foot swing data are displayed in Fig. 12. Data on left-hand movement is represented by solid lines, and information on foot movement is represented by dashed lines. Fig. 12's left panel displays SST-based marginal temporal coherences, while the right panel displays STFT-dependent marginal time consistencies. For both the left hand as well as foot activities sensory motor imaging information are distinguishable using the SST-based marginal time coherence.

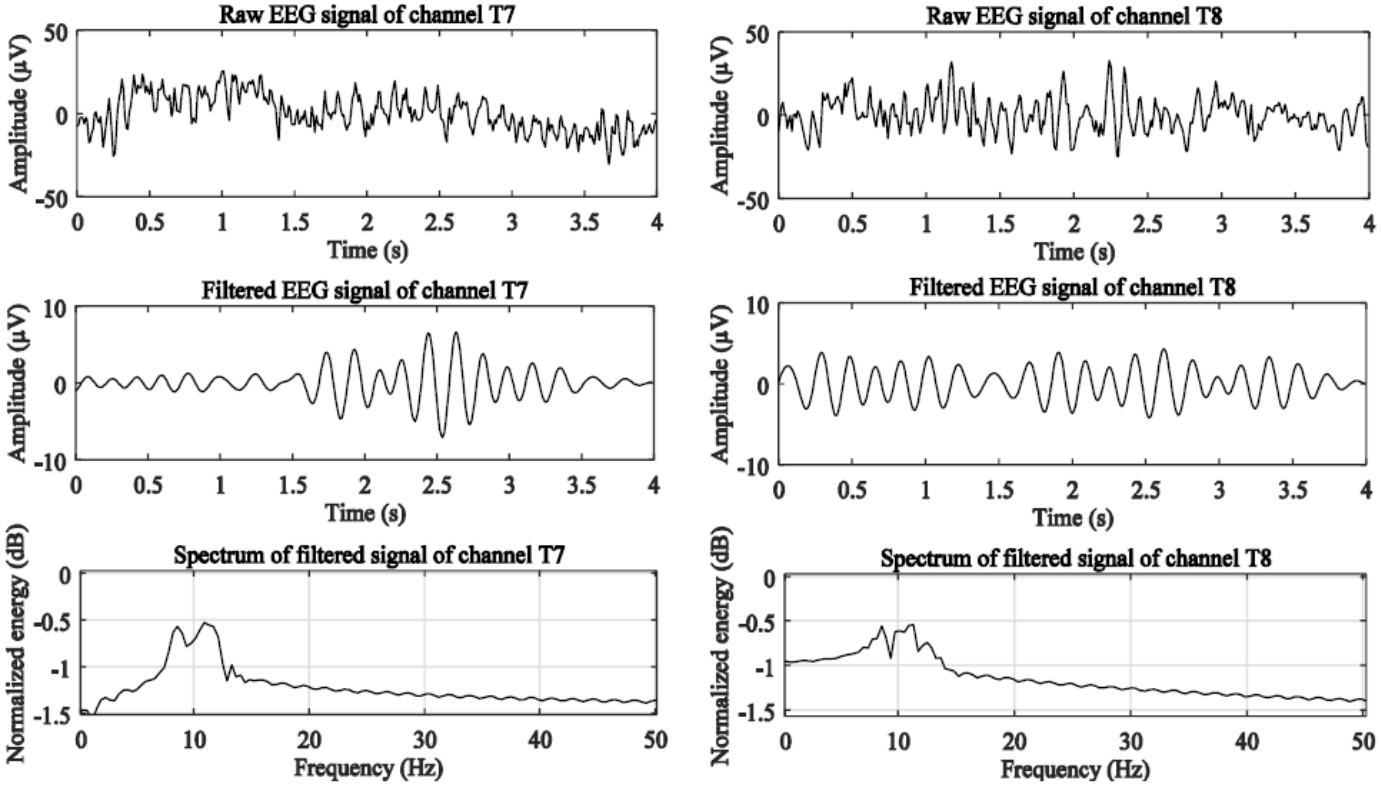

Fig. 7. Left hand movement data: first row is the raw EEG signals, second and third row are the filtered EEG signals and spectrums of the filtered component respectively.

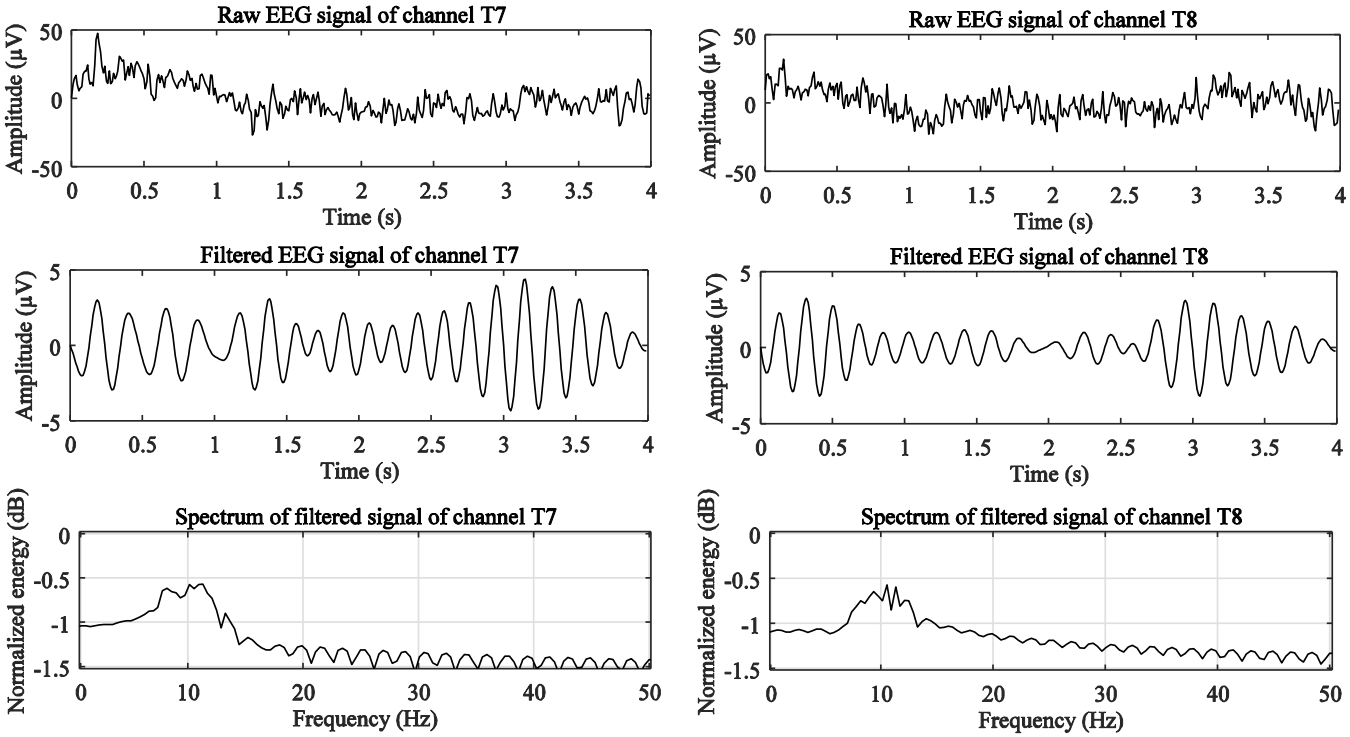

Fig. 8. Foot movement data: first row is the raw EEG signals, second and third row are the filtered EEG signals and spectrums of the filtered component respectively.

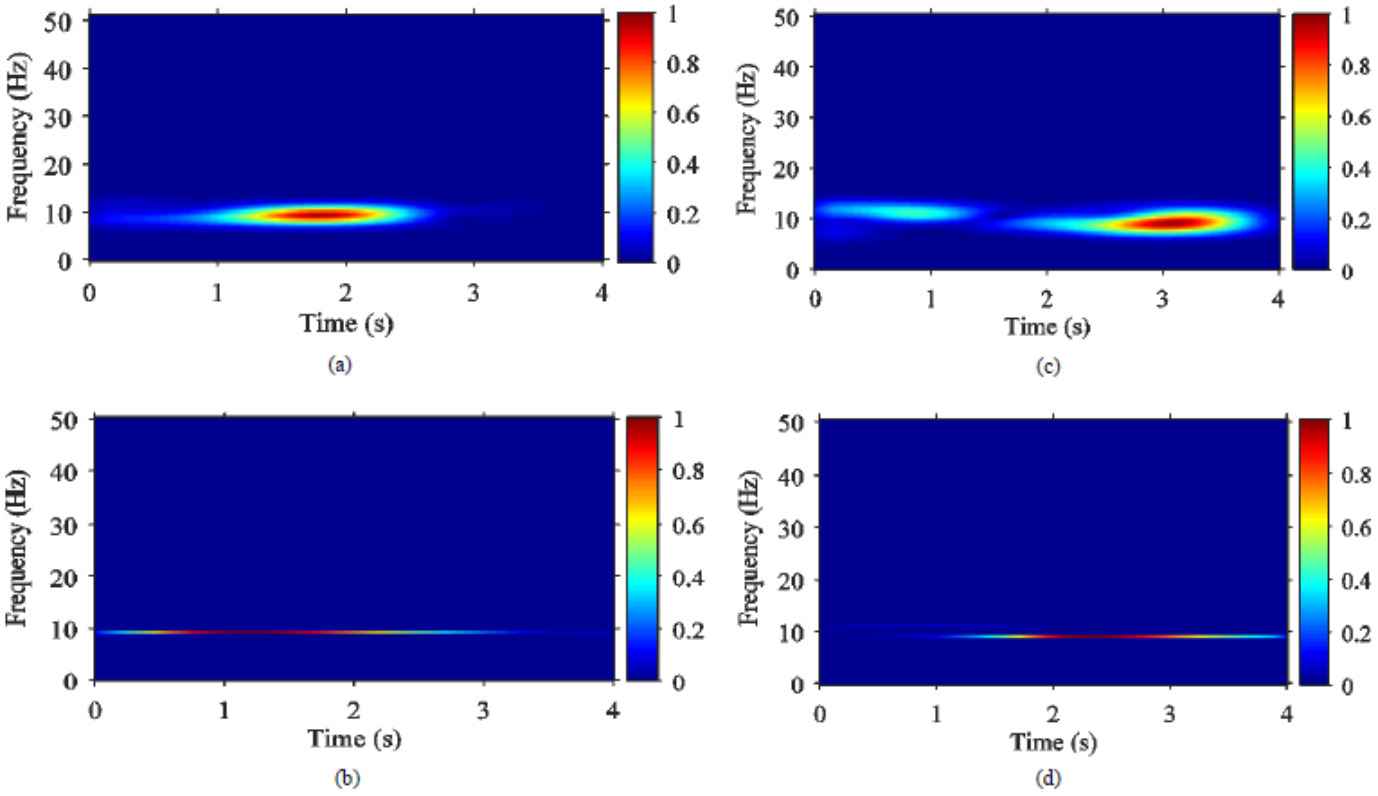

Fig. 9. TF coherence between channels T7 and T8 based on (a) STFT and (b) SST of left hand movement data, (c) STFT and (d) SST of foot movement data.

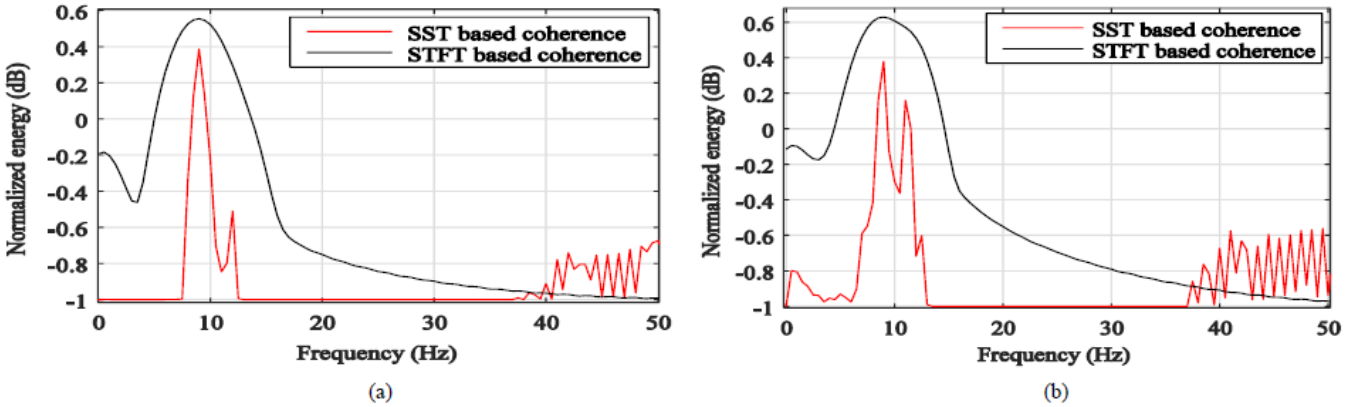

Fig. 10. Left hand action (a) as well as foot action (b) of channels T7 and T8 with marginal frequency consistencies.

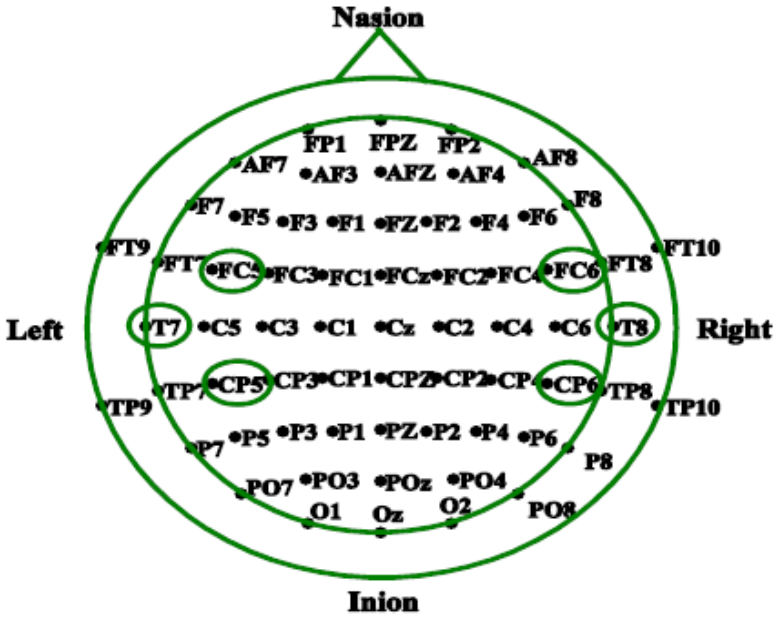

Fig. 11. The American EEG Society has standardized the electrode map of something like the 10/20 EEG system. For the dataset utilized in this experiment, the marked conductors T7, FC5, as well as CP5 beginning the left cerebral hemisphere and T8, FC6, as well as CP6 as of the right side of the brain were chosen.

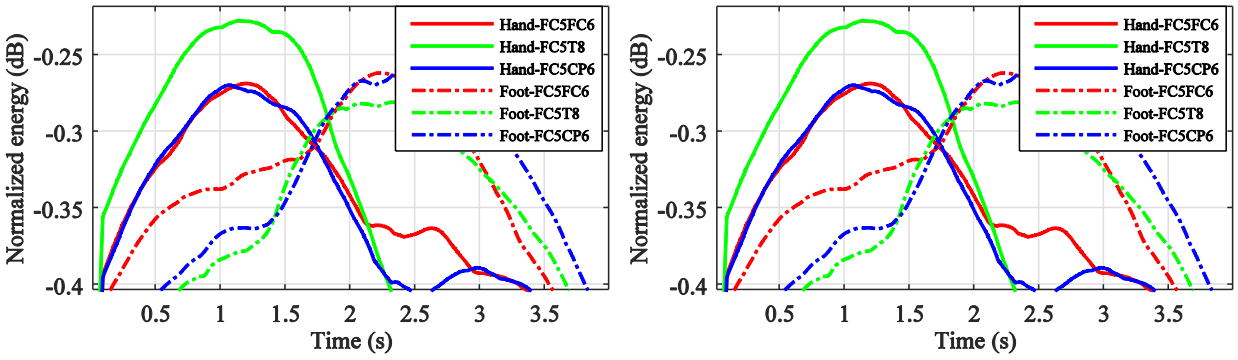

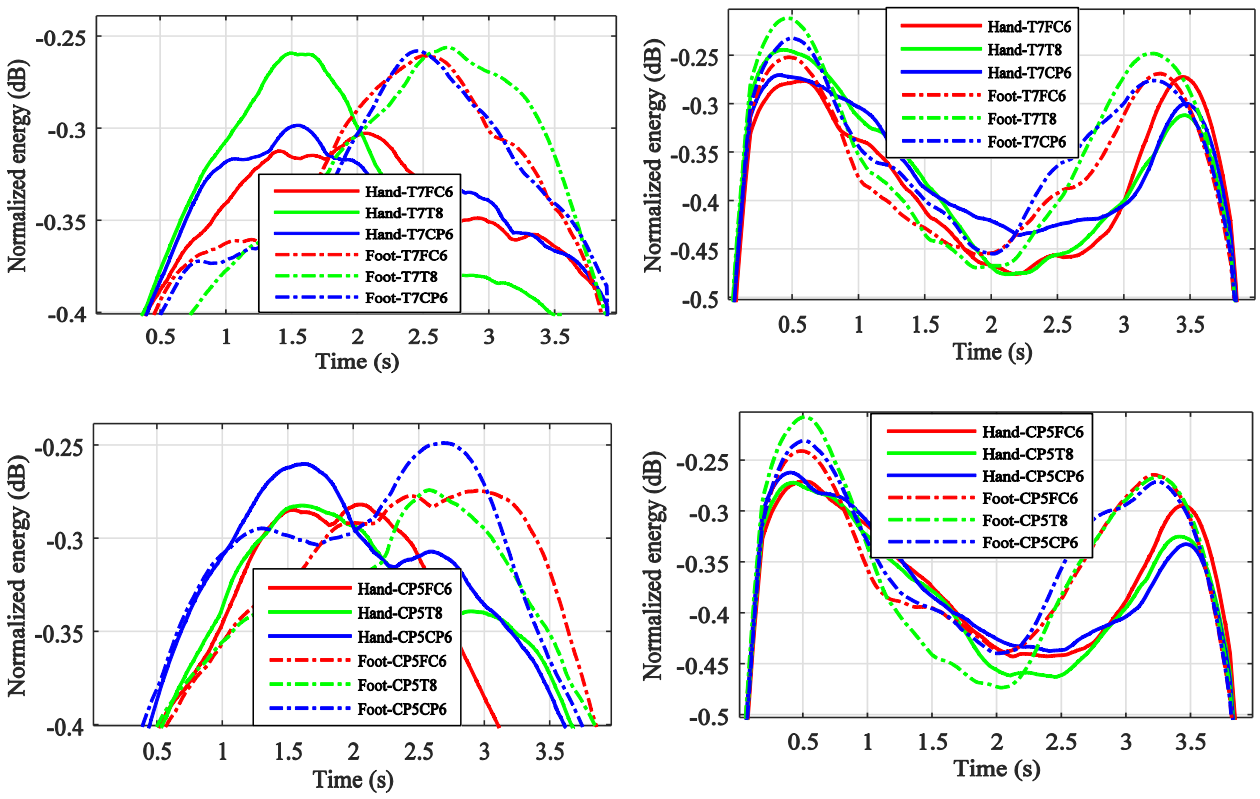

Fig. 12. Movement information for the left hand and foot for STFT-depended (right panel) and SST-based models (left panel) approaches exhibit a small amount of time coherence between distinct channel pairings.

IV. Discussion

EEG outputs are used in the research to examine how well SST performs in time-frequency illustration. Fig. 9 displays the TFR derived from left hand and foot movement data utilizing STFT and SST motor images. Fig. 10 shows, for left hand and left foot movement data, the energy related to the marginal frequency consistency. Although the SST-based technique shows acute localization of each frequency element within a relatively small band of frequencies, the marginal frequency coherence depended on STFT displays weak localization of frequency agents. The frequencies of 9 Hz and 11 Hz in Fig. 10(b) can be clearly distinguished using SST-based marginal frequency coherence, whereas they cannot be achieved using an STFT-dependent method. From now, SST-depended time-frequency consistency is better than STFT-based time-frequency coherence. The fundamental cause is that the employment of something like a window function for covering in STFT results in the introduction of cross-spectral energy, which causes the energy to spread over a broad range of frequencies. The TFR performance of the SST has been evaluated in our previous work [24]. This paper is a development of our earlier paper [24]. Our prior work is expanded upon in this one. In addition, the smoothing operations on the TFR, as well as BCI interpretation, are introduced in this paper. BCI can use marginal frequency coherence followed by marginal time coherence based on SST. The coherence value for left-hand movement data in the left panel of Fig. 12 is at its highest in the time range of 1-2 seconds, whereas the coherence value for foot movement data across all channel pairs is at its highest in the time range of two to three seconds. In the SST-based marginal temporal coherence, left-hand and foot measurement data are explicitly distinguished from one another. The marginal temporal coherence model based on STFT, however, does not exhibit this kind of selectivity (in the right panel). The main cause is the fact that the STFT has a fixed time-frequency window while the SST has a changeable one, making it difficult to accurately evaluate signals with broad bandwidths that fluctuate rapidly over time. Moreover, the STFT demands that the brain wave be stationary for a given time period, yet EEG signals exhibit non-stationary characteristics.

V. Conclusions

The analysis of the time-frequency (TF) consistency among two signals is offered in this work using an innovative approach. For each of the provided signals, the time-frequency densities of the crossed and auto spectrums are calculated. Then, using quasi smoothing agents, the spectral densities are smoothed. The TF coherence is calculated using smooth spectral densities for artificial signals with time-frequency representations based on STFT and SST. A genuine EEG signal with various motor images is used to test the suggested SST-based coherence estimate method. Comparing the two strategies' performances reveals that the SST-based approach is more effective than STFT at locating frequency contents with greater spatial precision. Then, using both SST and STFT-based coherences, marginal time coherences are computed. It is clearly shown that the STFT-depended

marginal time consistencies are incapable to distinguish among left hand and foot activity data, in contrast to the SST-depended marginal time coherences, which can. This implies that these marginal time coherences can enhance BCI design. In order to get greater performance, it is advised BCI designers to take these coherences as supplementary features when designing a BCI system.

Future study might explore brand-new combinations of features and feature selection, as well as the use of these features for BCI tasks other than motor imagery. Additionally, there is a need for work in the design of novel algorithms, including physiologically realistic error functions for EEG signal predictions for the complexity feature.

CONFLICTS OF INTEREST

The authors declare that there is no conflict of interest regarding the publication of this paper

REFERENCES

[1] Gregoriou GG, Gotts SJ, Zhou H, Desimone R (2009) High-Frequency, long-range coupling between prefrontal and visual cortex during attention. Sci. 324:1207–1210.

[2] Liang H, Bressler SL, Ding M, Desimone R, Fries P (2003) Temporal dynamics of attention-modulated neuronal synchronization in macaque V4. Neurocomputing 52:481–487.

[3] Brovelli A, Ding M, Ledberg A, Chen Y, Nakamura R, Bressler SL (2003) Beta oscillations in a large-scale sensorimotor cortical network: directional influences revealed by Granger causality. Proc. Natl. Acad. Sci. U.S.A. 101:9849–9854.

[4] Moller E, Schack B, Arnold M, Witte H (2001) Instantaneous multivariate EEG coherence analysis by means of adaptive high-dimensional autoregressive models. J. Neurosci. Methods 105:143-158.

[5] Daubechies I, Lu J, Wu H-T (2011) Synchrosqueezed wavelet transforms: an empirical mode decomposition-like tool. Appl. Computational Harmonic Anal. 30:243–261.

[6] Ahrabian A, Looney D, Stankovic L, Mandic DP (2015) Synchrosqueezing-based time-frequency analysis of multivariate data. Signal Process. 106:331-341.

[7] Auger F, Flandrin P, Lin Y-T, McLaughlin S, Meignen S, Oberlin T, Wu H-T (2013) Time-frequency reassignment and synchrosqueezing: an overview. IEEE Signal Process. Mag. 30: 32–41.

[8] Mehrkanoon S, Breakspear M, Daffertshofer A, Boonstra TW (2013) Non-identical smoothing operators for estimating time-frequency interdependence in electrophysiological recordings. EURASIP J. Advances Signal Process. 2013:1-16.

[9] Cohen E, Walden A (2010) A statistical study of temporally smoothed wavelet coherence. IEEE Trans. Signal Process. 58:2964–2973.

[10] Jin, J., Liu, C., Daly, I., Miao, Y., Li, S., Wang, X., & Cichocki, A. (2020). Bispectrum-based channel selection for motor imagery-based brain-computer interfacing. IEEE Transactions on Neural Systems and Rehabilitation Engineering, 28(10), 2153-2163.

[11] Suemitsu, K., & Nambu, I. (2023). Effects of Data Including Visual Presentation and Rest Time on Classification of Motor Imagery of Using Brain-Computer Interface Competition Datasets. IEEE Access. Jun 12

[12] Molla, M. K. I., Al Shiam, A., Islam, M. R., & Tanaka, T. (2020). Discriminative feature selection-based motor imagery classification using EEG signal. IEEE Access, 8, 98255-98265.

[13] Das, K., & Pachori, R. B. (2022). Electroencephalogram based motor imagery brain computer interface using multivariate iterative filtering and spatial filtering. IEEE Transactions on Cognitive and Developmental Systems.

[14] Li C, Liang M (2012) A generalized synchrosqueezing transform for enhancing signal time-frequency representation. Signal Process. 92: 2264–2274.

[15] Wu W-T, Flandrin P, Daubechies I (2011) One or two frequencies? The synchrosqueezing answers. Advances Adaptive Data Anal. 3:29–39.

[16] Tiesinga P, Fellous J-M, Sejnowski TJ (2008) Regulation of spike timing in visual cortical circuits. Nat. Rev. Neurosci. 9:97–107.

[17] Salinas E, Sejnowski TJ (2001) Correlated neuronal activity and the flow of neural information. Nat. Rev. Neurosci. 2:539–550.

[18] Fries P (2009) Neuronal gamma-band synchronization as a fundamental process in cortical computation. Annu. Rev. Neurosci. 32: 209-224.

[19] Lowet E, Roberts MJ, Bonizzi P, Karel J, De Weerd P (2016) Quantifying neural oscillatory synchronization: a comparison between spectral coherence and phase-locking value approaches. PloS one 11.

[20] Zhang ZG, Cai XL, Chan SC, Hu Y, Hu L, Chang CQ (2009) Time-frequency coherence analysis of multi-channel event-related potential using adaptive windowed Lomb periodogram. 4th International IEEE EMBS Conf. Neural Eng. 657-660.

[21] Brittain JS, Halliday DM, Conway BA, Nielsen JB (2007) Single-trial multiwavelet coherence in application to neurophysiological time series. IEEE Trans. Biomed. Eng. 54:854–862.

[22] McCreadie KA, Coyle DH, Prasad G (2013) Sensorimotor learning with stereo auditory feedback for a brain-computer interface. Med Biol Eng Comput 51: 285-293.

[23] Hadjidimitriou S, Zacharakis A, Doulgeris P, Panoulas K, Hadjileontiadis L, Panas S (2010) Sensorimotor cortical response during motion reflecting audiovisual stimulation: evidence from fractal EEG analysis. Med Biol Eng Comput 48: 561-572.

[24] Ali MS, Ferdous MJ, Hamid ME, Molla MKI, (2016) Time-frequency coherence of multichannel EEG signals: synchrosqueezing transform based analysis. International Journal of Computer Science Trends and Technology (IJCST) 4:40-48.

[25] Bang, J. S., Lee, M. H., Fazli, S., Guan, C., & Lee, S. W. (2021). Spatio-spectral feature representation for motor imagery classification using convolutional neural networks. IEEE Transactions on Neural Networks and Learning Systems, 33(7), 3038-3049.

[26] Saranyasoontorn K, Manuel L, Veers PS (2004) A comparison of standard coherence models for inflow turbulence with estimates from field measurements. J. Sol. Energy Eng. 126:1069-1082.

[27] Shovon, T. H., Al Nazi, Z., Dash, S., & Hossain, M. F. (2019, September). Classification of motor imagery EEG signals with multi-input convolutional neural network by augmenting STFT. In 2019 5th International Conference on Advances in Electrical Engineering (ICAEE) (pp. 398-403). IEEE.

[28] Xu, B., Zhang, L., Song, A., Wu, C., Li, W., Zhang, D., ... & Zeng, H. (2018). Wavelet transform time-frequency image and convolutional network-based motor imagery EEG classification. Ieee Access, 7, 6084-6093.